Received: 8 June 2020 | Revised: 3 October 2020 | Accepted: 5 October 2020
DOI: 10.1002/gj.4022

RESEARCH ARTICLE

WILEY

New U–Pb zircon ages of Nyong Complex meta-plutonites: Implications for the Eburnean/Trans-Amazonian Orogeny in southwestern Cameroon (Central Africa)

Sébastien Owona[1,2] | Lothar Ratschbacher[2] | Gulzar Afzal M[2] | Moussa Nsangou Ngapna[1] | Joseph Mvondo Ondoa[3] | Georges Emmanuel Ekodeck[3]

[1]Department of Earth Sciences, University of Douala, Douala, Cameroon
[2]Institute for Geology, TU Bergakademie Freiberg, Freiberg, Germany
[3]Department of Earth Sciences, University of Yaoundé I, Yaoundé, Cameroon

Correspondence
Sébastien Owona, Department of Earth Sciences, University of Douala, P.O. Box 24157, Douala, Cameroon.
Email: owonas@univ-douala.com

Funding information
German Academic Exchange Service

Handling Editor: I. Somerville

New LA–ICP–MS U–Pb zircon ages from the Nyong Complex of southwestern Cameroon—a part of the West Central African Fold Belt—trace Late Mesoarchean (∼2,850 Ma), Middle Palaeoproterozoic (∼2,080 Ma), and Neoproterozoic (∼605 Ma) events: Two meta-syenites and the protolith of an amphibolite are Late Mesoarchean; two meta-granodiorites are Middle Palaeoproterozoic; the amphibolite may have recrystallized in the Middle Palaeoproterozoic; all rocks are overprinted by the Neoproterozoic event. Integration with published data shows that our amphibolite sample has one of the oldest amphibolite-protolith ages (∼2,810 Ma) reported so far. It shares the Middle Palaeoproterozoic metamorphism/recrystallization with other, previously dated amphibolites. An earlier reported metamorphic zircon age (∼2,090 Ma) from eclogite is somewhat older than the regional Middle Palaeoproterozoic metamorphism/recrystallization ages (∼2,040 Ma) reported from amphibolites. Thus, the eclogite–amphibolite ages may date an exhumation process. A published charnockite age, interpreted as an Early Mesoarchean crystallization age, is older than the Late Mesoarchean meta-syenite and amphibolite-protolith dates; its Middle Palaeoproterozoic metamorphism/recrystallization age, however, is identical with the meta-granodiorites and amphibolites. The Neoproterozoic ages demonstrate the regional overprint of the Nyong Complex during this period. Integration of the Nyong Complex ages with published ones from the entire West Central African Fold Belt, and comparison with those from West Africa and South America, support their common origin from the Palaeoproterozoic collision between the Archean Congo and São Francisco shields.

KEYWORDS
Cameroon, LA–ICP–MS U–Pb zircon geochronology, Meso-Neoarchean protoliths, Nyong Complex, Palaeo- and Neoproterozoic reactivations

1 | INTRODUCTION

The Nyong Complex—also known as 'Lower Nyong unit', 'Nyong series', or 'Nyong Group' (Lasserre & Soba, 1976; Lerouge et al., 2006)—is the NW part of the Archean Congo Shield (De Wit, Stankiewicz, & Reeves, 2008), remobilized in the Palaeoproterozoic by the collision of the Congo and São Francisco shields during the Eburnean/Trans-Amazonian Orogeny (Figure 1a–c; e.g., Aguilar, Alkmim, Lana, & Farina, 2017; Alkmim & Wilson, 2017; Feybesse et al., 1998; Lerouge et al., 2006; Neves et al., 2006; Toteu, Van Schmus, Pénaye, & Nyobé, 1994). The Eburnean/Trans-Amazonian Orogeny can be classified—by its high-pressure and high-temperature metamorphic

This is an open access article under the terms of the Creative Commons Attribution License, which permits use, distribution and reproduction in any medium, provided the original work is properly cited.
© 2020 The Authors. *Geological Journal* published by John Wiley & Sons Ltd.

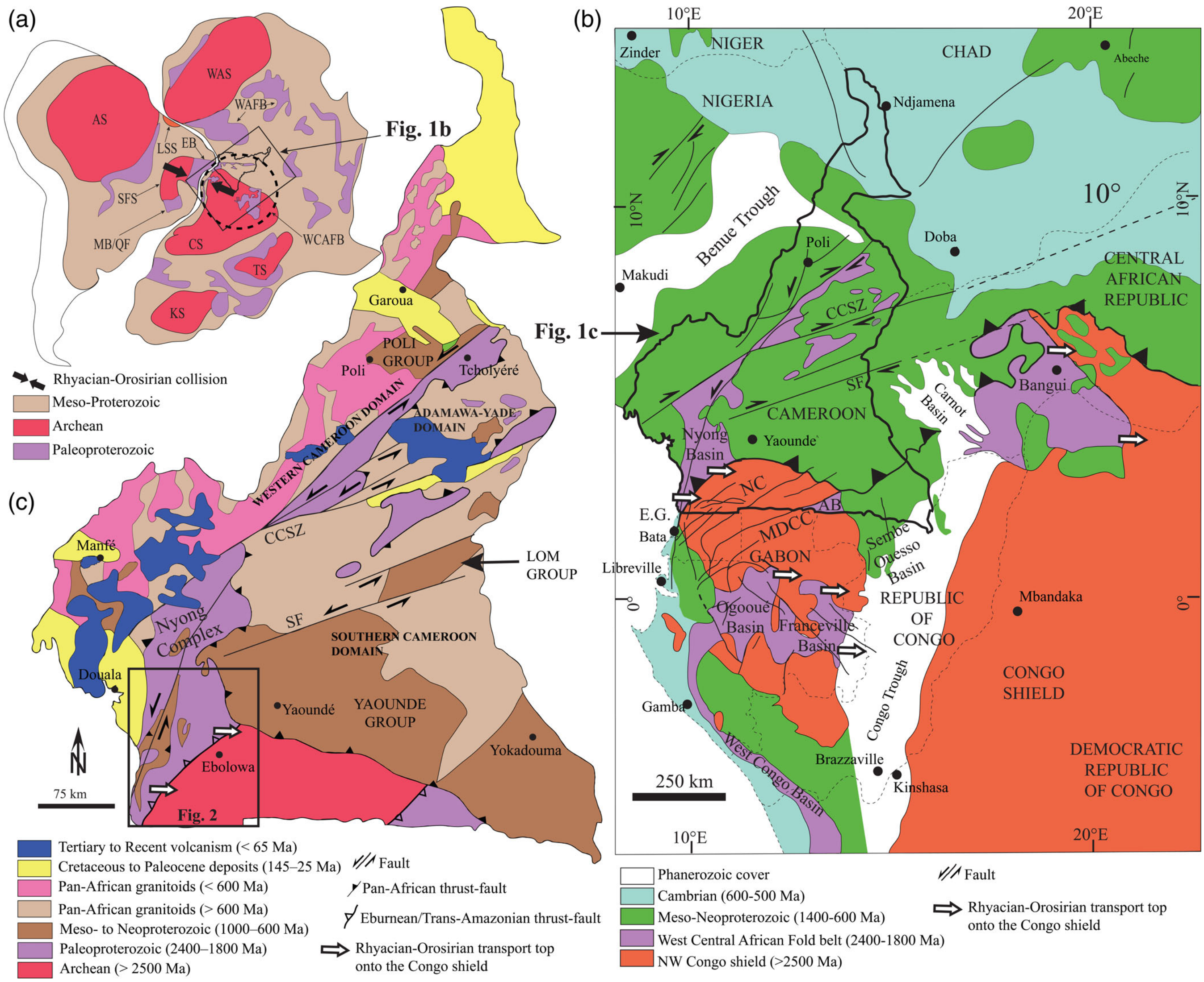

FIGURE 1 (a) South America–Africa fit, showing shields of western Gondwana (modified after Neves et al., 2006). (b) Geological sketch of Central Africa showing the regional extension of Palaeoproterozoic basins related to the West Central African Fold Belt (WCAFB). (c) Geological sketch of Cameroon, showing its Archean, Palaeo-, and Neoproterozoic basement and the Cretaceous–Cenozoic volcanic sedimentary cover (modified after Castaing, Feybesse, Thieblemont, Triboulet, & Chevremont, 1994; Ngako, Affaton, Nnangue, & Njanko, 2003; Owona, Mvondo Ondoa, & Ekodeck, 2013). AB, Ayna Basin; CCSZ, Central Cameroon Shear Zone; CS, Congo Shield; E.G., Equatorial Guinea; KS, Kalahari Shield; MDDCC, Mont de Cristal Complex; NC, Ntem Complex; SF, Sanaga Fault; SFS, São Francisco Shield; TS, Tanzania Shield; WAS, West African Shield [Colour figure can be viewed at wileyonlinelibrary.com]

mineral assemblages and the geochemistry of the related magmatic rocks—as a subduction–collision orogen. It stretches across Cameroon, the Central African Republic, Equatorial Guinea, and Gabon, forming the West Central African Fold Belt (WCAFB; Boniface, Schenk, & Appel, 2012; Houketchang Bouyo, Pénaye, Mouri, & Toteu, 2019; Feybesse et al., 1998; Loose & Schenk, 2018; Nga Essomba et al., 2019; Thiéblemont, Callec, Fernandez-Alonso, & Chène, 2018). Units equivalent to the Nyong Complex were mapped around the West African Shield, notably the Ashanti-Kumasi, Houndé, Lawra, Kédougou, Ouago-Fitini, and Reguibat belts (Kouamelan, Delor, & Peucat, 1997; Lambert-Smith, Lawrence, Müller, & Treloar, 2015; Parra-Avila et al., 2017; Peucat, Capdevila, Drareni, Mahdjoub, & Kahoui, 2005), and around the São Francisco Shield in Brazil, comprising the Eastern Bahia and Mineiro belts (Figure 1a; e.g., Aguilar et al., 2017; Alkmim & Wilson, 2017; Barbosa & Barbosa, 2017; Lopez, Cameron, & Jones, 2001; Neves et al., 2006).

The geochronologic studies published so far have shown that the igneous rocks of the Nyong Complex permit to trace its Archean core, its Palaeoproterozoic remobilization and growth during the Eburnean/Trans-Amazonian subduction and collision, and its Neoproterozoic Pan-African/Brasiliano reactivation (e.g., Caxito et al., 2020; Lerouge et al., 2006; Neves, Silva, & Bruguier, 2016; Nkoumbou, Barbey, Yonta-Ngouné, Paquette, & Villiéras, 2015; Oliveira et al., 2006, 2015; Silva, Ferreira, Lima, Sial, & Silva, 2015; Tchakounté et al., 2017; Toteu et al., 1994). U–Pb zircon geochronology is an appropriate method for timing the Nyong Complex evolution due to the high closure

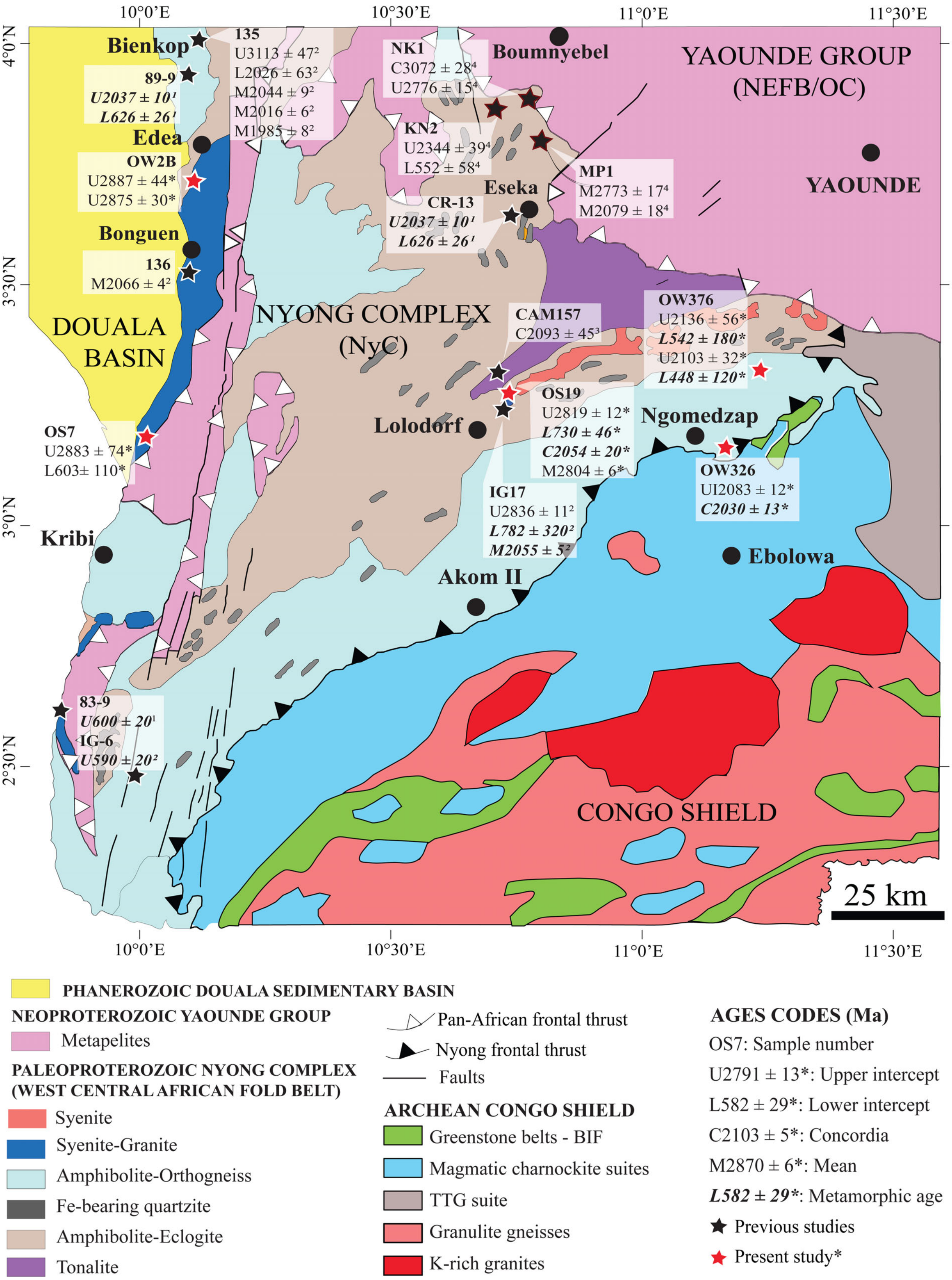

FIGURE 2 Geology of the Nyong Complex and related U–Pb zircon ages. NEFB, North Equatorial Fold Belt; OC, Oubanguide Complex. Published studies: 1, Toteu et al. (1994); 2, Lerouge et al. (2006); 3, Loose and Schenk (2018); 4, Nkoumbou et al. (2015). *Present study [Colour figure can be viewed at wileyonlinelibrary.com]

temperature of this system (e.g., Cherniak & Watson, 2001; Schoene, 2014). Herein, we provide new LA–ICP–MS U–Pb zircon ages from two meta-syenites, one amphibolite, and two meta-granodiorites of the Nyong Complex that highlight Mesoarchean protoliths, Eburnean/Trans-Amazonian orogenic overprint, and Pan-African/Brasiliano reactivation. Our data contribute to tie the Nyong Complex firmly into the Eburnean/Trans-Amazonian orogenic evolution and to define the duration of this orogeny in Central Africa more precisely.

2 | GEOLOGICAL SETTING

The basement of southwestern Cameroon comprises the Ntem, Nyong, and Oubanguide complexes (e.g., Owona et al., 2011). While the Ntem Complex comprises the Cameroonian part of the Archean Congo Shield, the Nyong Complex of the WCAFB represents those parts of the Archean Shield that were remobilized during the Eburnean/Trans-Amazonian Orogeny (Figures 1b,c and 2; e.g., Aguilar et al., 2017; Alkmim & Wilson, 2017; Barbosa & Barbosa, 2017; Feybesse et al., 1998; Neves et al., 2006; Pénaye et al., 2004). The Oubanguide Complex or North Equatorial Fold Belt, is the result of the Neoproterozoic collision between the Congo, West African, and Saharan shields (Figure 1a,b; Abdelsalam, Liégeois, & Stern, 2002; Castaing et al., 1994; Caxito et al., 2020; Feybesse et al., 1998).

Geochemical, petrographic, and structural data indicate that the Nyong Complex rocks comprise reworked/partially molten Archean crust (e.g., Lasserre & Soba, 1976; Nédélec, Minyem, & Barbey, 1993; Tchameni, Mezger, Nsifa, & Pouclet, 2001; Toteu et al., 1994). For example, neodymium-isotope data with T_{DM} ages of ~3,000 Ma corroborate the Archean origin of most protoliths (Pénaye et al., 2004). Petrographically, the Nyong Complex rocks comprise four main groups: (a) Meta-volcanic sedimentary rocks, probably remnants of greenstone belts, with orthopyroxene-bearing gneiss, garnet-rich amphibole-pyroxenite and related gneiss, banded iron formation, and mafic–ultramafic meta-volcanic rock; (b) migmatitic grey gneiss of tonalite–trondhjemite–granodiorite (TTG) composition; (c) syn- to late-tectonic (in respect to the Eburnean/Trans-Amazonian Orogeny) charnockite, (grano)dioritic augengneiss, granite, and syenite; (d) post-tectonic meta-dolerite (e.g., Chombong et al., 2017; Maurizot, Abessolo, Feybesse, Johan, & Lecompte, 1986; Owona et al., 2012; Pénaye et al., 2004). Structurally, the Nyong Complex is dominated by a NNE strike and shows a polyphase tectonic evolution. The meta-sedimentary rocks display a composite, sub-vertical foliation ($S_{1/2}$), marked by alternating ferromagnesian and leucocratic layers (e.g., Feybesse et al., 1998). The meta-granitoids contain the S_2 foliation. The entire Nyong Complex is dissected by NE-striking blastomylonitic shear zones (Figure 1b; e.g., Owona et al., 2011). The relative large variety of igneous rocks and their structural and often high-grade metamorphic overprint require a clear assessment of their protolith and metamorphic ages to solidly tie their origin and reworking to the multi-stage orogenic evolution of western Central Africa (e.g., Houketchang Bouyo, 2018; Houketchang Bouyo et al., 2019; Loose & Schenk, 2018; Tchakounté et al., 2017).

3 | SAMPLING AND ANALYTICAL METHODS

Our sampling strategy aimed for plutonic and metamorphic lithologies from the Nyong Complex that were not fully covered in previous studies, and to achieve a better understanding of the regional extent of the Eburnean/Trans-Amazonian Orogeny in Cameroon. To this end, we retrieved zircon grains from two meta-syenites (OS7 and OW2B), one amphibolite (OS19), and two meta-granodiorites (OW326, OW376) (Figure 2 and Table 1). We fragmented the rock samples using the high-voltage discharge SELFRAG facility at the TU Bergakademie Freiberg. Prior to mounting in epoxy, zircon concentrates were enriched with a Frantz magnetic separator, shaking tables, wet and dry sieving, wet panning, heavy liquids, and handpicking. Cathodoluminescence (CL) images were used to study the zircon textures that add to the interpretation of their geologic history (e.g., Corfu, Hanchar, Hoskin, & Kinny, 2003), and to avoid placing the laser ablation (LA) pits into possible multiple-age domains (e.g., core–rim boundaries) or inclusions. The inductively coupled plasma (ICP) mass spectrometry (MS) was performed at the Geochronology Laboratory of the Senckenberg Naturhistorische Sammlungen, Dresden, Germany. The laboratory uses a New Wave UP-193 Excimer Laser System coupled to a Thermo-Scientific Element 2 XR sector field LA–ICP–MS to collect U, Th, and Pb measurements for zircon grains. The data are not common Pb-corrected, and were generated using previously outlined protocols (Frei & Gerdes, 2009; Linnemann et al., 2011), with the caveat that data was processed using *Iolite* (Paton, Hellstrom, Paul, Woodhead, & Hergt, 2011). Laser spot sizes were 25 or 30 μm. Reported uncertainties were propagated by quadratic addition of the external reproducibility obtained from the reference zircon GJ-1 (~0.6 and 0.5–1.0% for $^{207}Pb/^{206}Pb$ and $^{206}Pb/^{238}U$, respectively) during individual analytical sessions and within-run precision of each analysis. To test the accuracy of the measurements and data reduction, we included the Plešovice zircon as a secondary reference in our analyses, which gave reproducibly ages of 335 ± 5 Ma, fitting with the results of Sláma et al. (2008) (see Horstwood et al., 2016 for details on the reference materials and data reporting; Table S1 provides the instrument settings of the geochronologic laboratory). We used *Isoplot* (Ludwig, 2008) to calculate, depending on context, the geologically most meaningful ages; these are either Concordia, weighted mean, or upper and lower intercept ages.

4 | SAMPLE LITHOLOGY

The meta-syenites show a metamorphic foliation and display a greyish-pink colour from outcrop- to hand-specimen scale (Figure 3a). Overall, they are leucocratic with a heterogeneous granoblastic texture of microcline (60–65%), actinolite (20–25%), green amphibole (<5%), plagioclase (<5%), and quartz (<5%) (Figure 3b). Microcline (0.05–5 mm) displays magmatic cores and recrystallized rims; recrystallized grains also occur in cracks and along shear zones. The green

TABLE 1 Sample locations, lithology, and U–Pb ages

Sample	Lithology	Latitude (N)	Longitude (E)	Age type	Age (Ma)	2s (Ma)	MSWD	Number of spots	Th/U median (range)	Age interpretation
OS7	Meta-syenite	03°10′35″	10°00′54″	Upper intercept	2,883	74	14.0	6	0.36 (0.26–0.49)	Crystallization
				Lower intercept	603	119				Metamorphic overprint
OW2B	Meta-syenite	03°42′34″	10°06′27″	Upper intercept	2,875	30	2.7	7	1.42 (0.12–1.91)	Crystallization[a]
				Lower intercept	430	67				Metamorphic overprint
OS19	Amphibolite	03°16′10″	10°44′08″	Upper intercept	2,819	12	3.8	46	0.49 (0.20–1.95)	Crystallization
				Lower intercept	730	46				Metamorphic overprint
				Weighted mean	2,804	6	1.1	22	0.48 (0.20–1.95)	Crystallization[b]
				Concordia	2,054	20	0.2	2	~2.3	Recrystallization/ Metamorphic overprint
OW326	Meta-granodiorite	03°09′27″	11°10′08″	Upper intercept	2,083	12	1.4	53	1.69 (0.52–3.57)	Crystallization
				Lower intercept	481	130				Metamorphic overprint
OW376	Meta-granodiorite	03°19′01″	11°14′10″	Upper intercept	2,103	32	1.0	15	0.78 (0.11–2.21)	Crystallization
				Lower intercept	448	120				Metamorphic overprint

[a]Eleven spots define a Discordia with upper and lower intercepts at 2,887 ± 44 Ma and 307 ± 120 Ma, respectively (MSWD = 9.6).
[b]Alternative date for this sample; we prefer the Upper Intercept Age.

amphibole (0.02–0.1 mm) blasts are derived from the uralitization of pyroxene. Quartz and plagioclase microblasts border magmatic plagioclase. Idiomorphic biotite occurs as inclusions in amphibole and as kinked blasts in the matrix. The 125–250 μm zircons are prismatic to round. They occur as inclusions in apatite (<0.5 mm) and opaques (<0.5 mm), feldspars, hornblende, and pyroxene.

The foliated amphibolite is dark green to black and contains thin layers of quartz-rich leucosome. It is holomelanocratic with a granoblastic texture that consists of green amphibole (70–75%), garnet (5–10%), biotite (5–10%), feldspar (5–10%), opaques (∼5%), and rare biotite, calcite, zircon, and epidote (Figure 3c,d). The amphibole (0.5–1 mm) occurs both as microblasts and porphyroblasts, often surrounding garnets. It is partly changed into epidote. Plagioclase (An_{45-75}) shows subhedral to euhedral, antiperthitic, and polysynthetic blasts (0.5–1.0 mm). Calcite and muscovite appear in the matrix. The 125–250 μm zircons are prismatic to round and occur as inclusions in opaques (<0.5 mm), feldspars, amphibole, and garnet.

The meta-granodiorites are pale green, foliated, and intercalated with felsic and fine-grained mafic layers. They are mesocratic, have a granoblastic texture, and consist of plagioclase (50–55%), quartz (20–25%), microcline (5–10%), biotite (<5%), and green amphibole (<5%); diopside, apatite, and zircon are accessories, and sericite, epidote, and calcite are secondary minerals (Figure 3e,f). Plagioclase (An_{20-40}) shows subhedral to euhedral, and antiperthitic blasts (0.5–1.0 mm); they are partially transformed into epidote. Quartz forms polycrystalline layers and anhedral blasts (0.5–2.0 mm) with undulose and patchy extinction. Biotite flakes (0.5–1.0 mm) are kinked and rich in opaques. Perthitic microcline occurs as recrystallized blasts (0.5–1.0 mm) in the matrix as does the green amphibole, which is retrogressed to epidote and calcite in outer zones and along cracks. Opaques, apatite, and calcite (<0.5 mm) occur as amoeboid to prismatic grains bordering green amphibole, and as euhedral and aligned microblasts in the matrix. Zircon (125–250 μm) occurs as inclusions in quartz, opaques, plagioclase, microcline, and amphibole.

5 | U–Pb ZIRCON DATING RESULTS

Figure 2 shows the sample locations in the geologic context. Table 1 summarizes the sample lithology, the sample locations, the interpreted U–Pb zircon ages, and the related Th/U values. Table S2 lists the U–Th–Pb measurements. Figures 4–6 visualize the U–Pb data as Concordia and—if useful—as weighted mean age (WMA) diagrams.

5.1 | Meta-syenites

We dated two meta-syenites. Sample OS7 displays a broad scatter of discordant analyses, indicating both Pb loss and common Pb contamination. Six analyses span a Discordia with an upper intercept (UI) at 2,883 ± 74 Ma and a lower intercept (LI) at 603 ± 110 Ma (2σ; MSWD = 14; Figure 4a). Although the high MSWD indicate non-analytical scatter, for example, the presence of common Pb also in these analyses, we interpret the UI to approximate the crystallization

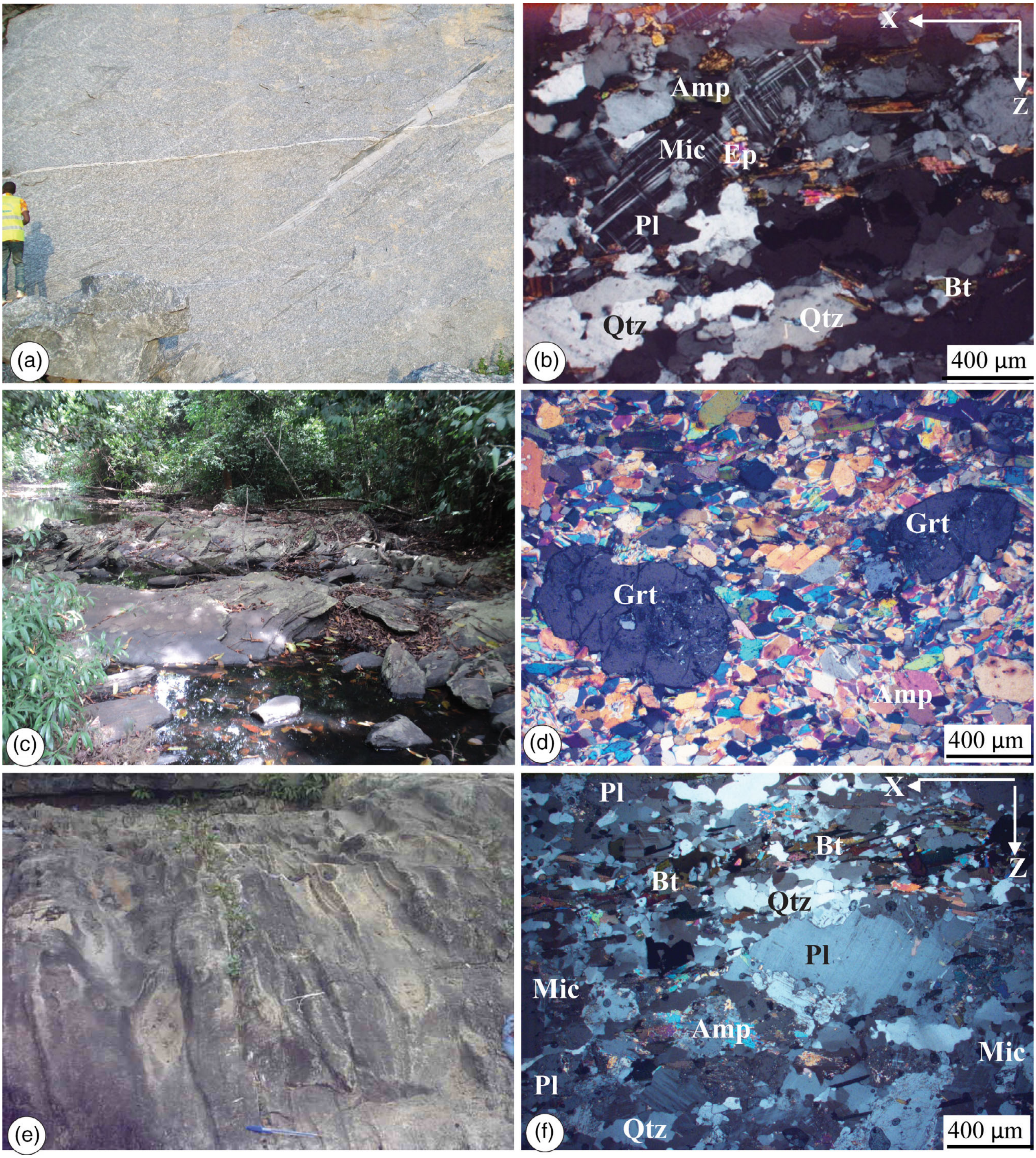

FIGURE 3 Sampled Nyong Complex lithologies. (a,b) Koukoue meta-syenite, (c,d) Lolodorf garnet-amphibolite, and (e,f) Akok meta-granodiorite. Left and right columns represent studied rocks in outcrop and thin section (in cross-polarized light). Note the oblique, sub-vertical foliation, and granoblastic texture in the studied meta-syenites and meta-granodiorites. Mineral abbreviations after Kretz (1983). Amp, amphibole; Bt, biotite; Ep, epidote; Grt, garnet; Mic, microcline; Pl, plagioclase; Qtz, quartz; Sph, sphene [Colour figure can be viewed at wileyonlinelibrary.com]

age and the LI as the period of the Pb loss event, for example, a thermal overprint; other regressions with fewer spot analyses yield lower MSWD, similar UI and LI dates, but higher uncertainties. The Th/U values (0.26–0.49, median = 0.36) indicate magmatic zircons. The CL images show blurred growth and sector zoning and commonly thin bright rims, too thin to be analysed; these features again imply overprinted igneous zircons.

Sample OW2B shows a similar, albeit less pronounced, scatter of spot dates. We fitted 2 Discordia to 7 respectively 11 analyses that yielded—on first order—similar intercepts. We consider the

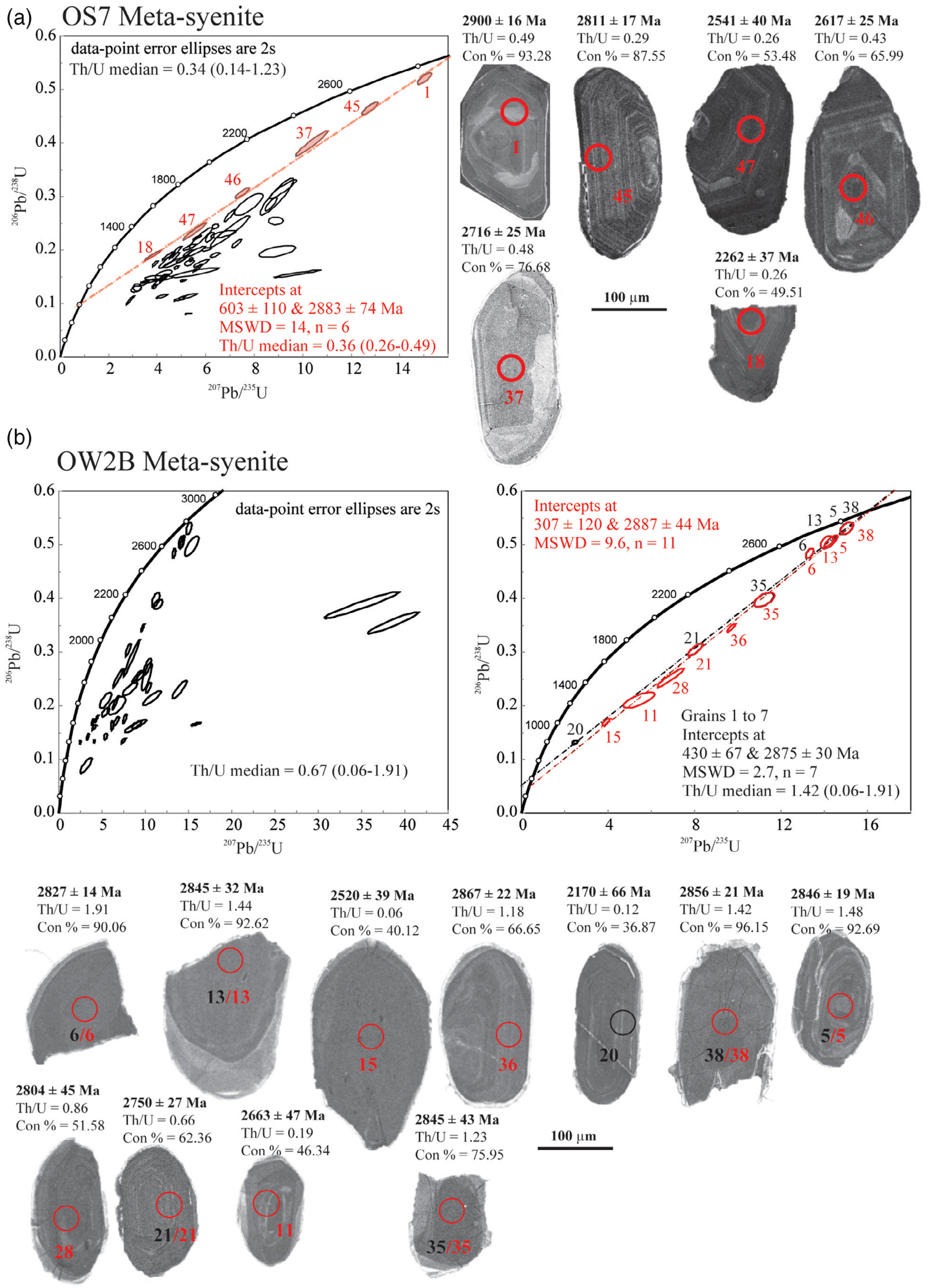

FIGURE 4 Concordia diagrams of the new U–Pb zircon geochronologic data and cathodoluminescence (CL) images of representative zircons. (a) Fifinda meta-syenite (OS7); (b) Koukoue meta-syenite (OW2B). Red and black numbers in the Discordia diagrams and CL images refer to the analysed spots used for the determination of the intercept ages given with same colours. Spot dates given next to the CL images are $^{207}Pb/^{206}Pb$ ages [Colour figure can be viewed at wileyonlinelibrary.com]

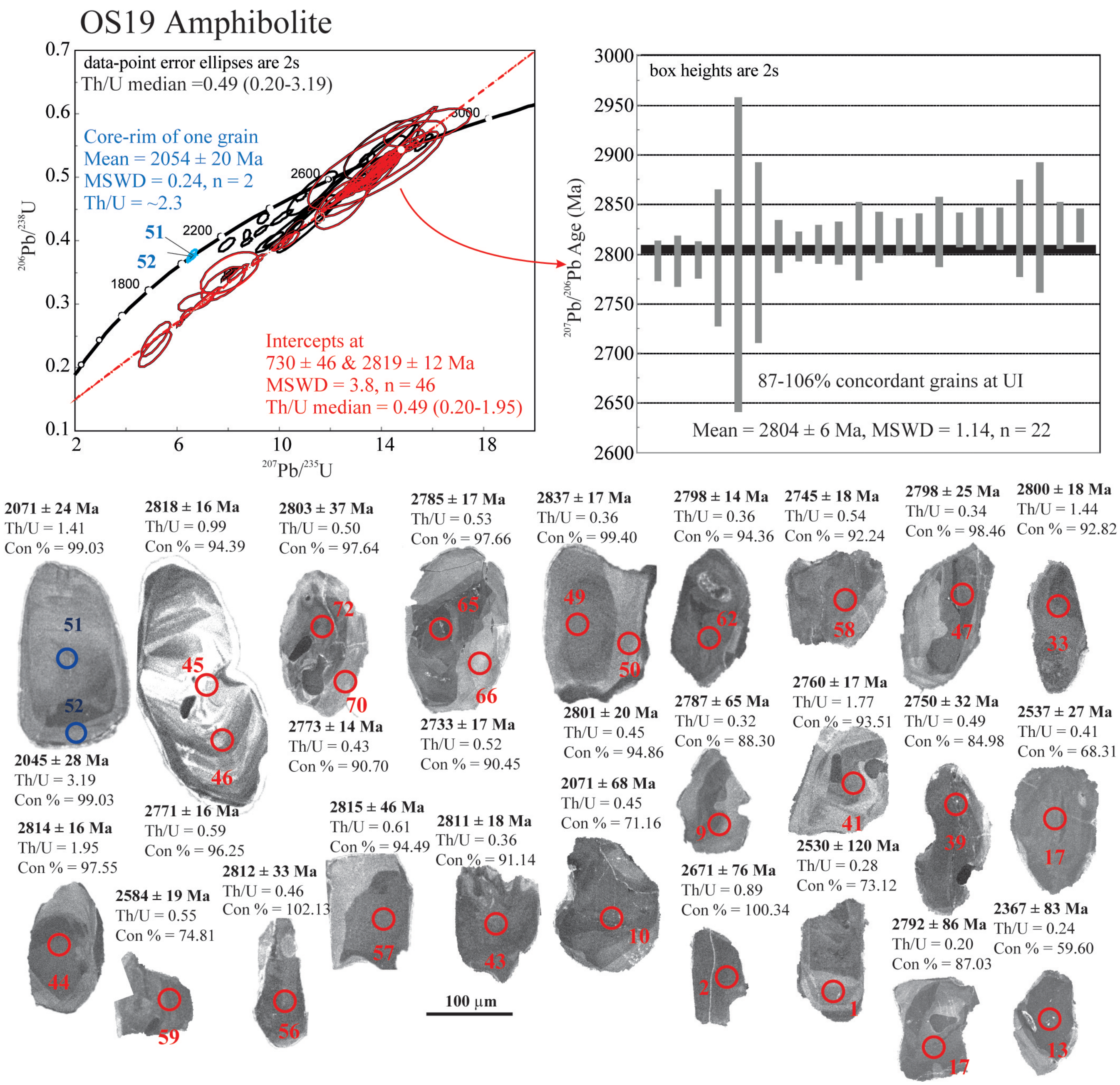

FIGURE 5 Concordia and weighted mean diagrams of the new U–Pb zircon geochronologic data and cathodoluminescence (CL) images of dated zircons of the Lolodorf amphibolite (OS19). Blue numbers in the Discordia diagram and CL images refers to the related mean age. Red numbers refer to analysed spots used for the determination of the intercept age. Spot dates given next to the CL images are $^{207}Pb/^{206}Pb$ ages [Colour figure can be viewed at wileyonlinelibrary.com]

one through 2,875 ± 30 Ma (UI) and 430 ± 67 Ma (LI, 2σ; MSWD = 2.7; Figure 4b) to approximate crystallization and overprint best. The Th/U values (0.12–1.91, median = 1.42) imply igneous zircons. The CL images—with strongly blurred growth zoning and, commonly, a thin bright rim—and the rounded edges of the zircon grains are similar to those of sample OS7. We interpret that the syenites crystallized in the latest Mesoarchean and were overprinted by a Neoproterozoic or younger thermal event.

5.2 | Amphibolite

Forty-six out of 72 analyses of amphibolite sample OS19 define UI and LI values of 2,819 ± 12 Ma and 730 ± 46 Ma (2σ; MSWD = 3.8; Figure 5). Twenty-two nearly concordant analyses (concordance in the $^{206}Pb/^{238}U$ &$^{207}Pb/^{206}Pb$ ages = 87–106%, median = 95%) yielded a WMA of 2,804 ± 6 Ma (2σ; MSWD = 1.14; Figure 5), similar to the UI age. Core and rim analyses of one concordant zircon yielded

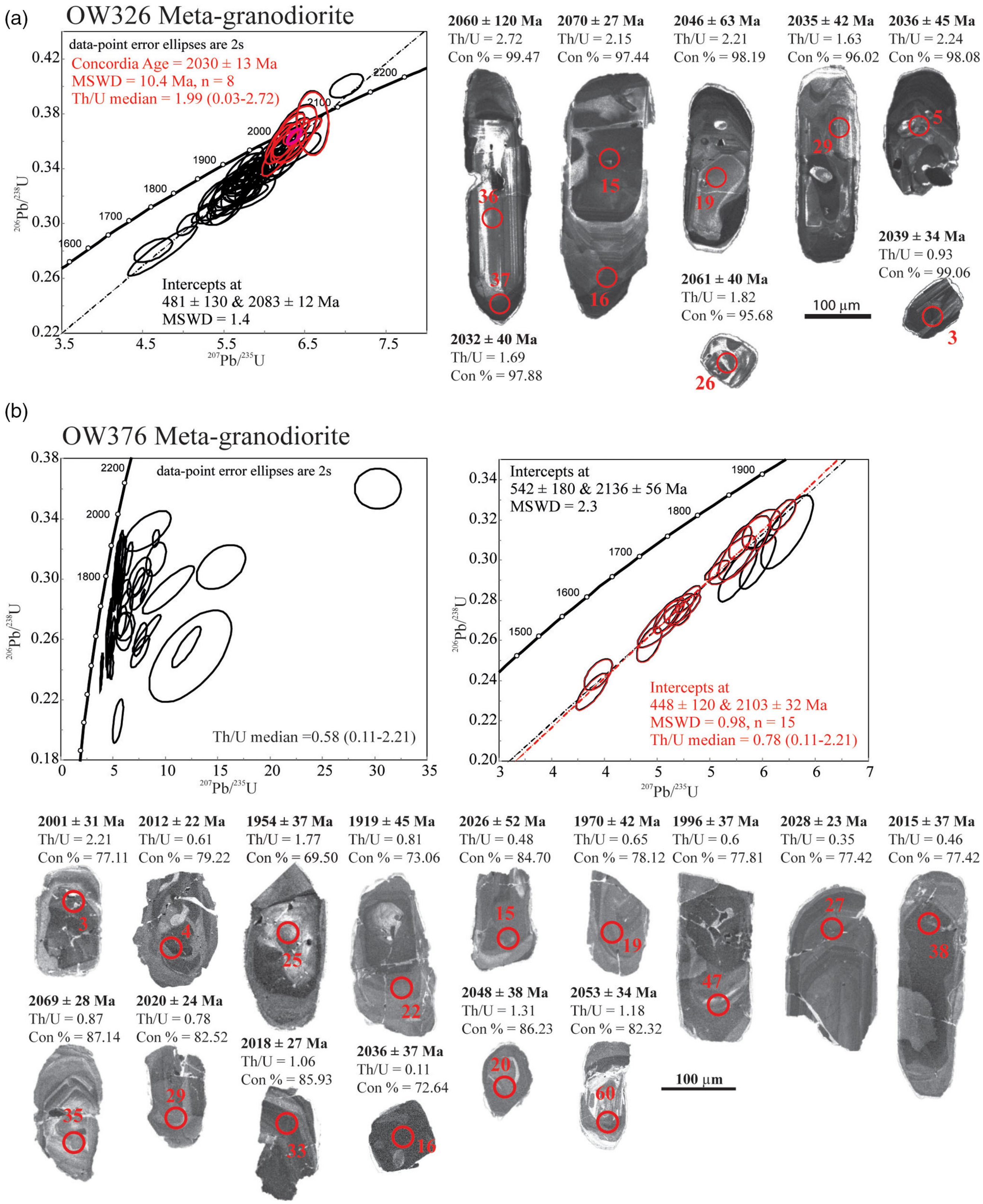

FIGURE 6 Concordia diagrams of the new U–Pb zircon geochronologic data and cathodoluminescence (CL) images of dated zircons. (a) Ngomedzap meta-granodiorite (OW326); (b) Abang Betsenga meta-granodiorite (OW376). Red and black spots in the Discordia diagrams refers to the Concordia and intercept ages given with same colours. Spot dates given next to the CL images are $^{207}Pb/^{206}Pb$ ages [Colour figure can be viewed at wileyonlinelibrary.com]

a WMA of 2,054 ± 20 Ma (2σ; MSWD = 0.24; Figure 5). All zircon grains have round or irregular shapes. Under CL, they overwhelmingly show textures typical for xenocrystic cores in magmatic and high-grade metamorphic rocks. The sector and fir-tree zoning, locally surrounding older zircon components, is characteristic for recrystallization in high-grade metamorphic rocks (Figure 5; cf. Corfu et al., 2003). We interpret the amphibolite to have crystallized in the latest Mesoarchean, overprinted by a Neoproterozoic thermal event. It is likely that there is a relict Palaeoproterozoic event.

5.3 | Meta-granodiorites

We dated two meta-granodiorites. Fifty-three analyses of sample OW326 yielded UI and LI dates at 2,083 ± 12 Ma and 481 ± 130 Ma (2σ; MSWD = 1.4; Figure 6a), respectively. Eight spots yielded a Concordia age of 2,030 ± 13 Ma, close to the UI age. The zircon grains are mostly prismatic with round edges. Under CL, they show—in the broad inner portions—sector and fir-tree zoning, typical for recrystallization in high-grade metamorphic rocks, blurred oscillatory magmatic zoning, typical for overprinted igneous rocks, often featureless rims, and thin and bright outermost rims, too thin to be analysed (Figure 6a).

Sample OW376 displays a broad scatter of discordant analyses indicating Pb loss and common Pb contamination. Fifteen analyses define a Discordia with UI and LI dates of 2,103 ± 32 Ma and 448 ± 120 Ma (2σ; MSWD = 0.98; Figure 6b). The zircon grains are similar to those of sample OW326, but the recrystallization features are more prominent. A large portion of the grains are broken but welded together by the same brightly luminescent material that makes up the tiny outermost rims. The meta-granodiorite dates are interpreted as Middle Palaeoproterozoic crystallization ages overprinted during the Neoproterozoic.

6 | DISCUSSION

Taken together, our new U–Pb zircon ages from the Nyong Complex trace Late Mesoarchean (~2,854 Ma, *n* = 3, weighted mean) and Middle Palaeoproterozoic (~2,079 Ma, *n* = 3) events; a Neoproterozoic (~607 Ma, *n* = 6) event is imprecisely defined. Both meta-syenites and the protolith of the amphibolite crystallized in the Late Mesoarchean; both meta-granodiorites crystallized in the Middle Palaeoproterozoic; the amphibolite likely recrystallized in the Middle Palaeoproterozoic. Our amphibolite sample yielded one of the oldest amphibolite-protolith crystallization ages (~2,819 Ma) reported so far. Nkoumbou et al. (2015) reported five older grains that yielded a Concordia age of 3,072 ± 28 Ma from a Nyong Complex amphibolite in the Boumnyebel area (Figure 2). Our amphibolite likely shares the Middle Palaeoproterozoic metamorphism/recrystallization (~2,054 Ma) with the amphibolites reported by Toteu et al. (1994) (~2,037 Ma). The metamorphic zircon age reported by Loose and Schenk (2018) from a Nyong Complex eclogite (~2,093 Ma) is somewhat older than the Middle Palaeoproterozoic amphibolite metamorphism/recrystallization (~2,039 Ma, summarizing all amphibole ages; Table S3). Thus, the eclogite–amphibolite ages may date a burial-exhumation process; this interpretation assumes a single metamorphic event, with zircon (neo) crystallization during eclogite-facies conditions and recrystallization during amphibolite-facies exhumation. All amphibolites record the Neoproterozoic overprint (~600 Ma).

Figure 7 integrates the new data with the published ones of the Nyong Complex; Table S3 lists the available dates and provides the relevant references. The pooled data bracket the duration of the magmatic and the metamorphic/recrystallization events in the Nyong Complex more precisely. It records a latest Mesoarchean/earliest Neoarchean (2,794 + 78/−21 Ma, *n* = 11, median) event, a Rhyacian (2,070 + 11/−26 Ma, *n* = 23) event, and an Ediacaran (613 + 13/−48 Ma, *n* = 21) event. For this calculation, we excluded five distinctly older crystallization ages (3,113–2,980 Ma, median = ~3,003 Ma) and seven distinctly younger crystallization ages (2,553–2,269 Ma, median = ~2,535 Ma) from the database of the Mesoarchean event; we excluded a single distinctly younger metamorphism/recrystallization age (~1891 Ma) from the Middle Palaeoproterozoic database; and we excluded five dates (972–730 Ma, median ~ 846 Ma), which also have large uncertainties, from the Neoproterozoic database. The excluded data may have geological significance, but they are disparate to the majority of the dates that define the three major events in the Nyong Complex. In contrast, Figure 7 contains all available dates.

First, our new and the published ages demonstrate the regional overprint of the Nyong Complex by the Pan-African/Brasiliano Orogeny during the Ediacaran–Cambrian West Gondwana amalgamation, marked by the collision of cratonic blocks, such as the West African–São Luís shields (Médio Coreaú–Dahomeyides–Gourma–West Tuareg Shield) and the São Francisco–Congo shields (Rio Preto–Riacho do Pontal–Sergipano–Yaoundé–Central African (e.g., Caxito et al., 2020). For comparison, the peak of the Pan-African overprint has been dated between 620–560 Ma (U–Pb zircon; Lerouge et al., 2006; Li et al., 2017; Toteu et al., 1994; Toteu, Penaye, & Djomani, 2004) and 613–586 Ma (EMP U–Th–Pb monazite; Li et al., 2017; Owona et al., 2011) in the Neoproterozoic Yaoundé Group of the Oubanguide Complex (North Equatorial Fold Belt). Second, our data and the published data demonstrate the reworking of Late Mesoarchean/Early Neoarchean crust, typical of the Congo Shield, during the Palaeoproterozoic Eburnean/Trans-Amazonian Orogeny. As implicit in its name, this orogeny spans, like the Pan-African/Brasiliano orogen, the Atlantic Ocean (e.g., Feybesse et al., 1998; Ledru, Johan, Milési, & Tegyey, 1994; Lerouge et al., 2006; Trompette, 1994). It encompasses the whole WCAFB (e.g., Feybesse et al., 1998; Lerouge et al., 2006; Loose & Schenk, 2018; Toteu et al., 1994), its South American equivalents, such as the Eastern Bahia and Mineiro belts (e.g., Aguilar et al., 2017; Alkmim & Wilson, 2017; Barbosa & Barbosa, 2017; Carvalho, Janasi, & Sayer, 2017), and its West African counterparts, the Ashanti-Kumasi, Houndé, Lawra, Kédougou, Ouago-Fitini, and Reguibat belts (e.g., Kouamelan et al., 1997; Lambert-Smith et al., 2015; Parra-Avila et al., 2017; Peucat et al., 2005).

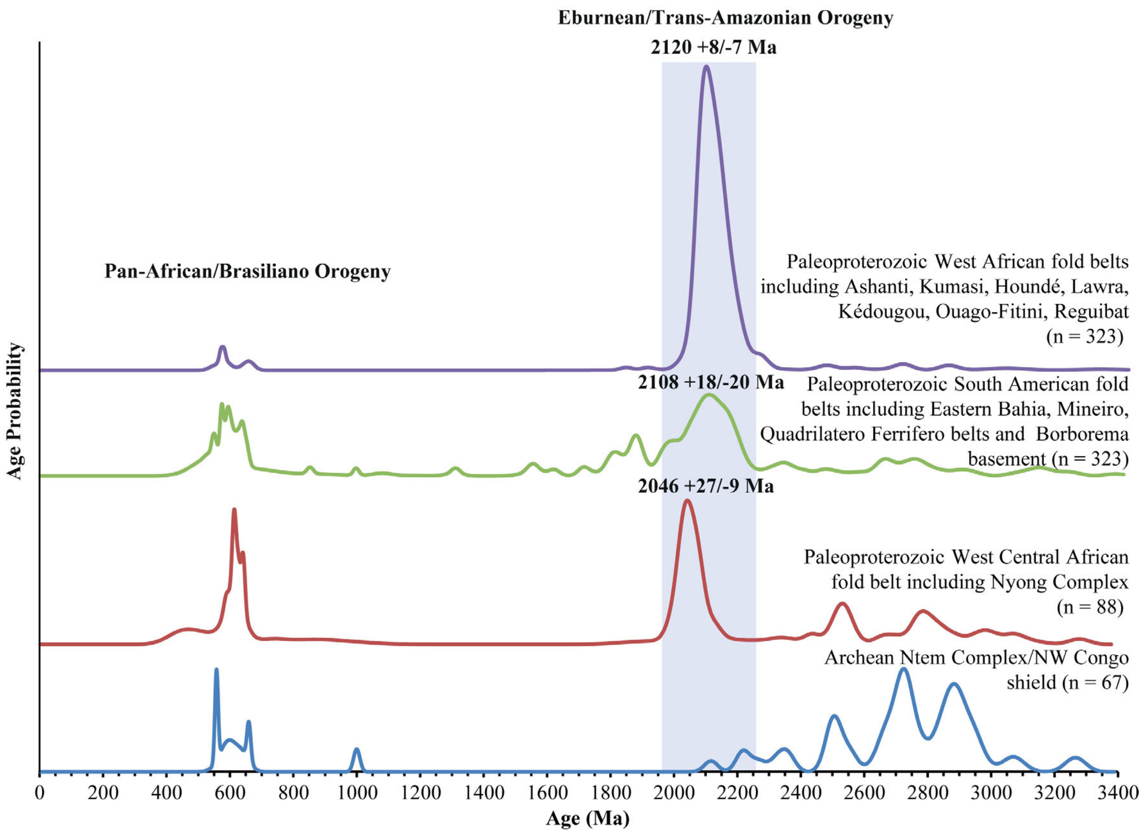

FIGURE 7 Normalized age probability diagrams summarizing the new and published U–Th–Pb ages from the West Central African Fold Belt (including the Nyong Complex), and those from the South American and West African equivalents. See Table S3 for the database and the text for discussion [Colour figure can be viewed at wileyonlinelibrary.com]

Figure 7 places our new ages into this super-regional orogenic evolution; the compilation includes the WCAFB and its South American and West African equivalents (Table S3 for the database and references). The age clusters correspond to the Archean protolith formation, the Palaeoproterozoic Eburnean/Trans-Amazonian Orogeny, and the Pan-African/Brasiliano reactivations. In detail, the evolution of the WCAFB started with dolerite magmatism within the Congo Shield, with a back-arc basin tholeiitic signature; it is interpreted as reflecting the pre-Eburnean extension and the onset of basin formation (e.g., Vicat et al., 1996; Vicat, Pouclet, Nkoumbou, & Seme Mouague, 1997). In Gabon, this magmatism includes the Kinguele metagabbro at ~2,777 Ma (Rb/Sr whole rock; Caen-Vachette, Vialette, Bassot, & Vidal, 1988) in the Mont de Cristal Complex, and the Koulamoutou amphibolite at ~2,672 Ma (Pb–Pb zircon; Caen-Vachette et al., 1988) in the Chaillu Complex. In the Nyong Complex of Cameroon, this tholeiitic magmatism is dated at ~2,628 Ma (Rb/Sr whole rock; Tchameni, Mezger, & Nsifa, 1995, 1996). In central Africa, the early extension is followed by the development of the Ogooué, Franceville, Nyong, West Congo, and Ayna basins of the WCAFB, between ~2,515 and 2,435 Ma (Figure 1b; Feybesse et al., 1998). These basins had older sources; for example, the Franceville-Ogooué basins include the Ndjole-series meta-sandstone, which received ~3,245 Ma-old detrital zircon grains (Pb–Pb; Feybesse et al., 1998); the Edea paragneiss of the Nyong Basin has detrital zircon grains as old as ~3,120 Ma (SHRIMP U–Pb; Lerouge et al., 2006). The basin strata were intermingled with the Archean basement rocks of the Congo Shield, when they were inverted during the Eburnean/Trans-Amazonian Orogeny.

The gneissic basement of the South American Mineiro Belt also reveals detrital zircons older than ~2,900 Ma (U–Pb zircon; Aguilar et al., 2017; Lana et al., 2013). Martin, Peucat, Sabate, and Cunha (1997), Santos Pinto, Peucat, Matin, and Sabaté (1998), and Martins (2014) described tonalite–trondhjemite–granodiorite complexes with Palaeo- to Mesoarchean U–Pb crystallization ages (3,400–3,100 Ma), among the oldest crustal pieces recognized so far in South America. The South American evolution also includes Neoarchean to Siderian sediment deposition and magmatism until ~2,300 Ma (U–Pb zircon, Aguilar et al., 2017). Similarly, the gneissic basement of the Palaeoproterozoic West African belts is older than ~2,700 Ma (U–Pb zircon; Kouamelan et al., 1997; Peucat et al., 2005). Lambert-Smith et al. (2015) described monzodiorites with Palaeo- to Mesoarchean U–Pb zircon crystallization ages (3,380–3,000 Ma), among the oldest crustal pieces recognized so far in West Africa.

The evolution of the WCAB continued with an accretion phase until ~2,145 Ma (Feybesse et al., 1998). This phase included minor introduction of juvenile material, represented by alkali-plutonism, such as the Abamie monzonitic granite at ~2,434 Ma (Pb–Pb zircon; Feybesse et al., 1998) and the Eteke tonalite at ~2,374 Ma (Pb–Pb zircon; Bonhomme, Gauthier-Lafaye, & Weber, 1982). This phase was accompanied by burial, crustal thickening, and migmatization in the Franceville-

Ogooué basin complexes, and in the Kribi quartzite of the Nyong Complex at ∼2,423 Ma, (U–Pb zircon; Lerouge et al., 2006). The margins of the Archean units, for example, the Chaillu, Mont de Cristals, and Ntem complexes, underwent renewed break-up until ∼2,145 Ma, forming the Ogooué, Franceville, Nyong, West Congo, and Ayna basins (Figure 1b; Feybesse et al., 1998). This phase was followed by the peak of the Eburnean/Trans-Amazonian Orogeny and the emplacement of tectonic nappes, such as the Franceville-Ogooué (∼2,130–2,120 Ma, Delhal & Ledent, 1976) and Nyong Nappes (∼2,050–2,030 Ma; Pénaye, Toteu, Van Schmus, & Nzenti, 1993; Toteu et al., 1994; Lerouge et al., 2006).

The WCAFB evolution ended with syn- to late-tectonic magmatism between ∼2,100 and 19,20 Ma. For example, the syn-tectonic one occurred at ∼2,040 Ma (Pb–Pb zircon; Feybesse et al., 1998) in the Franceville-Ogooué Complex and at ∼2,044 Ma in the Nyong Complex (Bienkop charnockite; Lerouge et al., 2006). We interpret our meta-granodiorites—emplaced at ∼2,103 and 2,083 Ma—as syn-tectonic with respect to the peak of metamorphism at ∼2,100–2,050 Ma, which probably extended until ∼1,985 Ma in the Nyong Complex (Feybesse et al., 1998; Lerouge et al., 2006; Loose & Schenk, 2018). Post-tectonic granitoids were emplaced, for example, as the ∼1,980 Ma Famougou granite in the Franceville-Ogooué Complex (Caen-Vachette et al., 1988), as the ∼1,941 Ma Alegre granodiorite and the ∼1,920 Ma Las Serras granodiorite in the West Congo Complex (Figure 1b; Maurin et al., 1991).

Our study—together with others in the Nyong Complex—define a relatively narrow range for the Eburnean/Trans-Amazonian Orogeny in southwestern Cameroon: ∼2,180–1,985 Ma (2,070 + 10/−26 Ma, median of 23 dates; see above). Pooling all dates from the WCAFB (including all dates from the Nyong Complex; Table S3) yields an identical range but a somewhat younger median: 2,046 + 27/−9 Ma (n = 33). Although the definition of the onset and termination of the Eburnean/Trans-Amazonian Orogeny is, in our opinion, more arbitrary than in the WCAFB, a grossly similar evolution is displayed in the South American fold belts (∼2,288–1,962 Ma, median of 95 dates = 2,109 + 18/−21 Ma), and the West African fold belts (∼2,290–1,850 Ma, median of 294 dates = 2,120 + 7/−9 Ma); this difficulty in the determination of the boundaries of the age ranges reflects the greater amount and variability of the available dates (Figure 7 and Table S3). The compilation may also hint to an asynchrony of the Eburnean/Trans-Amazonian Orogeny, having been earlier in the West African and South American fold belts than the WCAFB (Figure 7). These Palaeoproterozoic orogenic belts were reworked during the Pan-African/Brasiliano Orogeny at ∼592 + 21/−10 Ma (666–430 Ma, median of 80 dates from the WCAFB and its South American and West African equivalents; Table S3; compare to Caxito et al., 2020).

7 | CONCLUSIONS

New and published U–Pb zircon ages allow us to tighten the tectonic evolution of the Nyong Complex of southwestern Cameroon. First, the pooled data bracket the duration of the magmatic and the metamorphic/recrystallization events in the Nyong Complex more precisely. Its evolution comprised latest Mesoarchean/earliest Neoarchean (median 2,794 + 78/−21 Ma) protoliths, remobilization of the NW Congo Shield during its collision with São-Francisco Shield associated with the Eburnean/Trans-Amazonian Orogeny that peaked with the emplacement of Rhyacian (2,070 + 11/−26 Ma) syn-tectonic meta-granodiorites, and ended with the Ediacaran (613 + 13/−48 Ma) reactivation during the Pan-African/Brasiliano Orogeny, associated with the collision between the Congo and West African shields. Second, we relate the Middle Palaeoproterozoic evolution of Nyong Complex to the Eburnean/Trans-Amazonian of the West Central African and West African fold belts, and their South American equivalents, such as the Eastern Bahia and Mineiro belts. The dates from first West African (2,120 + 7/−9 Ma) and South American (2,109 + 18/−21 Ma) fold belts are on first order identical, those of the West Central African Fold Belt (2,046 + 27/−9 Ma) are younger; this may hint to a regional asynchrony or time progression of the Eburnean/Trans-Amazonian Orogeny. However, the variable database—more variable but more extensive in the West African and South American fold belts—makes the definition of the boundaries and the age ranges for these comparisons dependent on future studies. Similarly, although the eclogite and amphibolite ages in the Nyong Complex likely bracket a burial-exhumation process (∼2,090–2,040 Ma), the full timing of the prograde and retrograde paths of the Eburnean metamorphism in western Central Africa needs more age dating. Third, almost all rocks of the Nyong Complex were overprinted during the Neoproterozoic Pan-African Orogeny. This calls for more work on its temperature–pressure evolution and its comparison with the Oubanguide Complex/North Equatorial Fold Belt with its dominantly Neoproterozoic evolution.

ACKNOWLEDGEMENTS

Sébastien Owona acknowledges grants from the DAAD (German Academic Exchange Service), support by the TU Bergakademie Freiberg, and constructive suggestions of Elson Oliveira and Ian Somerville. Open Access funding enabled and organized by Projekt DEAL [Correction added on 30 March 2021, after first online publication: Projekt DEAL funding statement has been added.]

PEER REVIEW

The peer review history for this article is available at https://publons.com/publon/10.1002/gj.4022

DATA AVAILABILITY STATEMENT

The data that supports the findings of this study are available in the supplementary material of this article.

ORCID

Sébastien Owona https://orcid.org/0000-0002-1345-9107

REFERENCES

Abdelsalam, G. M., Liégeois, L., & Stern, R. J. (2002). The Saharan metacraton. *Journal of African Earth Sciences*, *34*, 119–136.

Aguilar, C., Alkmim, F. F., Lana, C., & Farina, F. (2017). Paleoproterozoic assembly of the São Francisco Craton, SE Brazil: New insights from U–Pb titanite and monazite dating. *Precambrian Research*, *289*, 95–115.

Alkmim, F., & Wilson, T. (2017). The Paleoproterozoic mineiro belt and the Quadrilátero Ferrífero. In *São Francisco Craton, Eastern Brazil*, Regional geology reviews (pp. 71–94). Cham, Switzerland: Springer International Publishing.

Barbosa, J. S. F., & Barbosa, R. G. (2017). The Paleoproterozoic Eastern Bahia orogenic domain. In M. Heilbron, U. G. Cordani, & F. F. de Alkmim (Eds.), *São Francisco Craton, Eastern Brazil*, Regional geology reviews (pp. 57–69). Cham, Switzerland: Springer International Publishing.

Bonhomme, M. G., Gauthier-Lafaye, F., & Weber, F. (1982). An example of Lower Proterozoic sediments: The Francevillian in Gabon. *Precambrian Research*, *18*, 87–102.

Boniface, N., Schenk, V., & Appel, P. (2012). Paleoproterozoic eclogites of MORB-type chemistry and three Proterozoic orogenic cycles in the Ubendian Belt (Tanzania): Evidence from monazite and zircon geochronology, and geochemistry. *Precambrian Research*, *192–195*, 16–33.

Caen-Vachette, M., Vialette, Y., Bassot, J.-P., & Vidal, P. (1988). Apport de la géochronologie à la connaissance de la géologie gabonaise. *Chronique de Recherche Minière*, *491*, 35–54.

Carvalho, B. B., Janasi, V. A., & Sayer, E. W. (2017). Evidence for Paleoproterozoic anatexis and crustal reworking of Archean crust in the São Francisco Craton, Brazil: A dating and isotopic study of the Kinawa migmatite. *Precambrian Research*, *29*, 98–118.

Castaing, C., Feybesse, J. L., Thieblemont, D., Triboulet, C., & Chevremont, P. (1994). Paleogeographical reconstructions of the Pan-African/Brasiliano orogen: Closure of an oceanic domain or intracontinental convergence between major blocks. *Precambrian Research*, *69*, 327–344.

Caxito, F. A., Santos, L. C. M. L., Ganade, C. E., Bendaoud, A., Fettous, E.-H., & Houketchang Bouyo, M. (2020). Toward an integrated model of geological evolution for NE Brazil–NW Africa: The Borborema Province and its connections to the Trans-Saharan (Benino-Nigerian and Tuareg shields) and Central African orogens. Special session, "A tribute to Edilton Santos, a leader in Precambrian Geology in Northeastern Brazil", edited by A.N. Sial and V.P. Ferreira. *Brazilian Journal of Geology*, *50*(2), 1–38. https://doi.org/10.1590/2317-4889202020190122

Cherniak, D. J., & Watson, E. B. (2001). Pb diffusion in zircon. *Chemical Geology*, *172*, 5–24.

Chombong, N. N., Suh, C. E., Lehmann, B., Vishiti, A., Ilouga, D. C., Shemang, E. M., … Kedia, A. C. (2017). Host rock geochemistry, texture and chemical composition of magnetite in iron ore in the Neoarchaean Nyong unit in southern Cameroon. *Applied Earth Science*, *126*(3), 129–145.

Corfu, F., Hanchar, J. M., Hoskin, P. W. O., & Kinny, P. (2003). Zircon: Atlas of zircon textures J. M. Hanchar & P. W. O. Hoskin (Eds.), *Zircon: Mineralogical Society of America reviews in mineralogy and geochemistry* (Vol. 53, pp. 468–500). Zircon: Geochemical Society, Mineralogy and Geochemistry.

De Wit, M. J., Stankiewicz, J., & Reeves, C. (2008). Restoring Pan-African–Brasiliano connections: More Gondwana control, less Trans-Atlantic corruption. In R. J. Pankurst, R. A. J. Trouw, B. B. Brito Neves, & M. J. de Wit (Eds.), *West Gondwana: Pre-Cenozoic correlations across the South Atlantic region*, Geological Society of London, London, Special Publications (Vol. 294, pp. 399–412). London: Geological Society of London.

Delhal, J., & Ledent, D. (1976). Age et évolution comparée des gneiss migmatitiques prézadiniens des régions de Boma et de Mpozo-Tombagadio (Bas-Zaïre). *Annales de la Société Géolologique de Belgique*, *99*, 165–187.

Feybesse, J. L., Johan, V., Triboulet, C., Guerrot, C., Mayaga-Minkolo, F., Bouchot, V., & Eko N'dong, J. (1998). The West Central African Belt: A model of 2.5–2.0 Ga accretion and two-phase orogenic evolution. *Precambrian Research*, *87*, 161–216.

Frei, D., & Gerdes, A. (2009). Precise and accurate in situ U–Pb dating of zircon with high sample throughput by automated LA–SF–ICP–MS. *Chemical Geology*, *261*(3), 261–270.

Horstwood, M. S. A., Košler, J., Gehrels, G., Jackson, S. E., McLean, N. M., Paton, C., … Schoene, B. (2016). Community-derived standards for LA–ICP–MS U–(Th–)Pb geochronology – Uncertainty propagation, age interpretation, and data reporting. *Geostandards and Geoanalytical Research*, *40*(3), 311–332.

Houketchang Bouyo, M. (2018). Comment on "The Adamawa–Yadé Domain, a piece of Archaean crust in the Neoproterozoic Central African Belt (Bafia area, Cameroon) by Tchakounté et al., 2017" (Precambrian Research 299, 210–229). *Precambrian Research*, *305*, 504–507.

Houketchang Bouyo, M., Pénaye, J., Mouri, H., & Toteu, S. F. (2019). Eclogite facies meta-basites from the Paleoproterozoic Nyong Group, SW Cameroon: Mineralogical evidence and implications for a high-pressure metamorphism related to a subduction zone at the NW margin of the Archean Congo Craton. *Journal of African Earth Sciences*, *149*, 215–234.

Kouamelan, A. N., Delor, C., & Peucat, J. J. (1997). Geochronological evidence for reworking of Archean terrains during the Early Proterozoic (2.1 Ga) in the western Cote d'Ivoire (Man Rise-West African Craton). *Precambrian Research*, *86*, 177–199.

Kretz, R. (1983). Symbols of rock-forming minerals. *American Mineralogy*, *68*, 277–279.

Lambert-Smith, J. S., Lawrence, D. M., Müller, W., & Treloar, P. J. (2015). Palaeotectonic setting of the south-eastern Kédougou-Kéniéba Inlier, West Africa: New insights from igneous trace element geochemistry and U–Pb zircon ages. *Precambrian Research*, *274*, 110–135.

Lana, C., Alkmim, F. F., Armstrong, R., Scholz, R., Romano, R., & Nalini, H. A., Jr. (2013). The ancestry and magmatic evolution of Archean TTG rocks of the Quadrilátero Ferrífero Province, southeast Brazil. *Precambrian Research*, *231*, 157–173.

Lasserre, M., & Soba, B. (1976). Age libérien de granodiorites et des gneiss à pyroxène du Cameroun méridional. *Bulletin du Bureau de Recherche Géologique et Minière 2e série, section*, *IV*(I), 17–32.

Ledru, P., Johan, V., Milési, J. P., & Tegyey, M. (1994). Markers of the last stages of the Palaeoproterozoic collision: Evidence for a 2 Ga continent involving circum-South Atlantic provinces. *Precambrian Research*, *69*, 169–191.

Lerouge, C., Coherie, A., Toteu, S. F., Pénaye, J., Milesi, J. P., Tchameni, R., … Deloule, E. (2006). Shrimp U–Pb zircon age evidence for Paleoproterozoic sedimentation and 2.05 Ga syntectonic plutonism in the Nyong Group, south-western Cameroon: Consequences for the Eburnean–Trans Amazonian Belt of NE Brazil and Central Africa. *Journal of African Earth Sciences*, *44*(4–5), 413–427.

Li, X.-H., Chen, Y., Tchouankoue, J. P., Liu, C.-Z., Li, J., Ling, X.-X., … Liu, Y. (2017). Improving geochronological framework of the Pan-African orogeny in Cameroon: New SIMS zircon and monazite U–Pb age constraints. *Precambrian Research*, *294*, 307–321.

Linnemann, U., Ouzegane, K., Drareni, A., Hofmann, M., Becker, S., Gärtner, A., & Sagawe, A. (2011). Sands of West Gondwana: An archive of secular magmatism and plate interactions—A case study from the Cambro–Ordovician section of the Tassili Ouan Ahaggar (Algerian Sahara) using U–Pb–LA–ICP–MS detrital zircon ages. *Lithos*, *123*(1), 188–203.

Loose, D., & Schenk, V. (2018). 2.09 Ga old eclogites in the Eburnean–Trans Amazonian orogeny of southern Cameroon: Significance for a Paleoproterozoic plate tectonics. *Precambrian Research*, *304*, 1–11.

Lopez, R., Cameron, K. L., & Jones, N. W. (2001). Evidence for Paleoproterozoic, Grenvillian, and Pan-African age Gondwanan crust beneath northeastern Mexico. *Precambrian Research*, *107*(3–4), 195–214.

Ludwig, K. R. (2008). Isoplot 3.70. A geochronological toolkit for Microsoft Excel. *Berkeley Geochronology Center Special Publication*, *4*, 1–76.

Martin, H., Peucat, J. J., Sabate, P., & Cunha, J. C. (1997). Crustal evolution in the Early Archaean of South America: Example of the Sete Voltas Massif, Bahia State, Brazil. *Precambrian Research*, *82*, 35–62.

Martins, A. A. M. (Org.). (2014). *Projeto Brumado–Condeúba* (p. 67p). Salvador, Brazil: Serviço Geológico do Brasil, CPRM.

Maurin, J. C., Boudzoumou, F., Djama, L. M., Gioan, P., Michard, A., Mpemba-Boni, J., … Vicat, J. P. (1991). La chaîne protérozoïque ouest Congolienne et son avant-pays au Congo: nouvelles données géochronologiques et structurales, implications en Afrique centrale. *Compte Rendu de l'Académie des Sciences, Paris*, *312*, 1327–1334.

Maurizot, P., Abessolo, A., Feybesse, A., Johan, J. L., & Lecompte, P. (1986). Etude et prospection minière au Sud – Ouest Cameroun. Synthèse des travaux de 1978–1985. In *Rapport BRGM*, *85 CNRS 066, Orléans* p. 274, Orléans: Rapport, Bureau de recherches géologiques et minier.

Nédélec, A., Minyem, D., & Barbey, P. (1993). High P-high T anatexis of Archean tonalitic grey gneisses: The Eseka migmatites, Cameroon. *Precambrian Research*, *62*, 191–205.

Neves, S. P., Bruguier, O., Vauchez, A., Bosch, D., Rangel da Silva, J. M., & Mariano, G. (2006). Timing of crust formation, deposition of supracrustal sequences, and Trans Amazonian and Brasiliano metamorphism in the East Pernambuco Belt (Borborema Province, NE Brazil): Implications for western Gondwana assembly. *Precambrian Research*, *149*, 197–216.

Neves, S. P., Silva, J. M. R., & Bruguier, O. (2016). The transition zone between the Pernambuco–Alagoas Domain and the Sergipano Belt (Borborema Province, NE Brazil): Geochronological constraints on the ages of deposition, tectonic setting and metamorphism of metasedimentary rocks. *Journal of South American Earth Sciences*, *72*, 266–278.

Nga Essomba, T. P., Ganno, S., Tanko Njiosseu, E. L., Ndema Mbongue, J. L., Kamguia Woguia, B., Soh Tamehe, L., … Nzenti, J. P. (2019). Geochemical constraints on the origin and tectonic setting of the serpentinized peridotites from the Paleoproterozoic Nyong series, Eseka area, SW Cameroon. *Acta Geochimica*, *38*, 1–19.

Ngako, V., Affaton, P., Nnangue, J. M., & Njanko, T. (2003). Pan-African tectonic evolution in central and southern Cameroon: Transpression and transtension during sinistral shear movements. *Journal of African Earth Sciences*, *36*, 207–214.

Nkoumbou, C., Barbey, P., Yonta-Ngouné, C., Paquette, J. L., & Villiéras, F. (2015). Pre-collisional geodynamic context of the southern margin of the Pan-African Fold Belt in Cameroon. *Journal of African Earth Sciences*, *99*, 245–260.

Oliveira, E. P., Bueno, J. F., McNaughton, N. K., Silva Filho, A. F., Nascimento, R. S., & Donatti-Filho, J. P. (2015). Age, composition, and source of continental arc- and syn-collision granites of the Neoproterozoic Sergipano Belt, Southern Borborema Province, Brazil. *Journal of South American Earth Sciences*, *58*, 257–280.

Oliveira, E. P., Toteu, S. F., Araújo, M. N. C., Carvalho, M. J., Nascimento, R. S., Bueno, J. F., … Basilici, G. (2006). Geologic correlation between the Neoproterozoic Sergipano Belt (NE Brazil) and the Yaoundé schist belt (Cameroon, Africa). *Journal of African Earth Sciences*, *44*, 470–478.

Owona, S., Mvondo Ondoa, J., & Ekodeck, G. E. (2013). Evidence of quartz, feldspar and amphibole crystal plastic deformations in the Paleoproterozoic Nyong complex shear zones under amphibolite to granulite conditions (West Central African Fold Belt, SW Cameroon). *Journal of Geography and Geology*, *5*(3), 186–201.

Owona, S., Mvondo Ondoa, J., Ratschbacher, L., Mbola Ndzana, S. P., Tchoua, M. F., & Ekodeck, G. E. (2011). The geometry of the Archean, Paleo- and Neoproterozoic tectonics in the Southwest Cameroon. *Comptes Rendus Geosciences*, *343*, 312–322.

Owona, S., Tichomirowa, M., Ratschbacher, L., Mvondo Ondoa, J., Youmen, D., Pfänder, J. A., … Affaton, P. (2012). New igneous (zircon Pb/Pb) and metamorphic (Rb/Sr) ages in the Neoproterozoic Yaoundé Group (Cameroon, Central Africa): Consequences for the orogenic evolution north of The Congo Craton. *International Journal of Earth Sciences*, *101*(7), 1689–1703.

Parra-Avila, L. A., Kemp, A. I. S., Fiorentini, M. L., Belousova, E., Baratoux, L., Block, S., … McCuaiga, T. C. (2017). The geochronological evolution of the Paleoproterozoic Baoulé–Mossi Domain of the Southern West African Craton. *Precambrian Research*, *300*, 1–27.

Paton, C., Hellstrom, J., Paul, B., Woodhead, J., & Hergt, J. (2011). Iolite: Freeware for the visualization and processing of mass spectrometric data. *Journal of Analytical Atomic Spectrometry*, *26*(12), 2508–2518.

Pénaye, J., Toteu, S. F., Tchameni, R., Van Schmus, W. R., Tchakounté, J., Ganwa, A., … Nsifa, E. N. (2004). The 2.1 Ma West Central African Belt in Cameroon: Extension and evolution. *Journal of African Earth Sciences*, *39*, 159–164.

Pénaye, J., Toteu, S. F., Van Schmus, W. R., & Nzenti, J. P. (1993). U/Pb and SM/Nd preliminary geohronologic data on the Yaounde series, Cameroon: Re-interpretation of granulitic rocks as the suture of a collision in the "Centrafrican Belt". *Compte Rendu de l'Académie des Sciences, Paris, Série II*, *317*, 789–794.

Peucat, J.-J., Capdevila, R., Drareni, A., Mahdjoub, Y., & Kahoui, M. (2005). The Eglab Massif in the West African Craton (Algeria), an original segment of the Eburnean orogenic belt: Petrology, geochemistry and geochronology. *Precambrian Research*, *136*, 309–352.

Santos Pinto, M. A., Peucat, J. J., Matin, H., & Sabaté, P. (1998). Recycling of the Archaean continental crust: The case study of the Gavião Block, Bahia, Brazil. *Journal of South American Earth Sciences*, *11*, 487–498.

Schoene, B. (2014). 4.10: U–Th–Pb geochronology. In *Treatise on geochronology. The crust* (Vol. 4, pp. 341–378). Princeton, NJ: Elsevier.

Silva, T. R., Ferreira, V. P., Lima, M. M. C., Sial, A. N., & Silva, M. R. (2015). Synkinematic emplacement of the magmatic epidote bearing major Isidoro tonalite-granite batholith: Relicts of an Ediacaran continental arc in the Pernambuco–Alagoas Domain, Borborema Province, NE Brazil. *Journal of South American Earth Sciences*, *64* (1), 1–13.

Sláma, J., Košler, J., Condon, D. J., Crowley, J. L., Gerdes, A., Hanchar, J. M., … Whitehouse, M. J. (2008). Plešovice zircon—A new natural reference material for U–Pb and Hf isotopic microanalysis. *Chemical Geology*, *249*, 1–35.

Tchakounté, J., Eglinger, A., Toteu, S. F., Zeh, A., Nkoumbou, C., Mvondo-Ondoa, J., … Barbey, P. (2017). The Adamawa–Yadé Domain, a piece of Archaean crust in the Neoproterozoic Central African Orogenic Belt (Bafia area, Cameroon). *Precambrian Research*, *299*, 210–229.

Tchameni, R., Mezger, K., & Nsifa, E. N. (1995). Archaean and Early Proterozoic evolution of The Congo Craton (Southern Cameroon). *EUG VIII*, *Terra Abstracts*, *7*, 102.

Tchameni, R., Mezger, K., & Nsifa, E. N. (1996). Geochemical and Nd–Sr isotope composition of the Archaean Ntem granitoids (Southern-Cameroon): Evidence for rapid crustal growth. *Journal Conference Abstracts*, 616.

Tchameni, R., Mezger, K., Nsifa, N. E., & Pouclet, A. (2001). Crustal origin of Early Proterozoic meta-syenites in The Congo Craton (Ntem complex), South Cameroon. *Lithos*, *57*, 23–42.

Thiéblemont, D., Callec, Y., Fernandez-Alonso, M., & Chène, F. (2018). A geological and isotopic framework of Precambrian terrains in Western Central Africa: An introduction. In S. Siegesmund, M. Basei, P. Oyhantçabal, & S. Oriolo (Eds.), *Geology of Southwest Gondwana* (pp. 107–132). Berlin: Springer International Publishing .

Toteu, S. F., Penaye, J., & Djomani, Y. P. (2004). Geodynamic evolution of the Pan-African Belt in Central Africa with special reference to Cameroon. *Canadian Journal of Earth Sciences*, *41*, 73–85.

Toteu, S. F., Van Schmus, W. R., Pénaye, J., & Nyobé, J. B. (1994). U/Pb and Sm/Nd evidence for Eburnean and Pan-African high-grade metamorphism in cratonic rocks of southern of Cameroon. *Precambrian Research*, *67*, 321–347.

Trompette, R. (1994). *Geology of western Gondwana (2000–500 Ma). Pan-African–Braziliano aggregation of South America and Africa*. Rotterdam, the Netherlands: A.A. Balkema.

Vicat, J. P., Léger, J. M., Nsifa, K. E., Piguet, P., Nzenti, J. P., Tchameni, R., & Pouclet, A. (1996). Distinction au sein du craton congolais du Sud-Ouest du Cameroun, de deux épisodes doléritiques initiant les cycles orogéniques éburnéen (Paléoprotérozoique) et panafricain (Néoprotérozoique). *Compte Rendu de l'Académie des Sciences, Paris, Série IIa*, *323*, 575–582.

Vicat, J. P., Pouclet, A., Nkoumbou, C., & Seme Mouague, A. C. (1997). Le volcanisme fissural Néoprotérozoique des séries du Dja inférieur, de Yokadouma (Cameroun) et de Nola (RCA) - Signification géotectonique. *Compte Rendu de l'Académie des Sciences, Paris*, *325*, 671–677.

SUPPORTING INFORMATION

Additional supporting information may be found online in the Supporting Information section at the end of this article.

How to cite this article: Owona S, Ratschbacher L, Afzal M G, Nsangou Ngapna M, Mvondo Ondoa J, Ekodeck GE. New U–Pb zircon ages of Nyong Complex meta-plutonites: Implications for the Eburnean/Trans-Amazonian Orogeny in southwestern Cameroon (Central Africa). *Geological Journal*. 2021;56:1741–1755. https://doi.org/10.1002/gj.4022